

WESTERN REGION TECHNICAL ATTACHMENT  
NO. 87-45  
November 3, 1987

"REVERSE" DEFORMATION ZONE

The relationship between deformation and frontogenesis and the resultant secondary circulation is well known and has recently been discussed in WRTA 86-15. The ascending portion of the secondary circulation has been tied to enhanced cloudiness and precipitation on the warm air side of the frontogenetical zone. Figure 1 shows the resultant secondary circulation across the zone of intensifying horizontal baroclinicity. In many cases, such as that discussed in WRTA 86-15, with a closed low over the southwest and split flow along the west coast, low level warm air advection will exist to the east of the low. If a short wave has passed over the ridge to the north, frontogenesis will occur where low level cold advection east of the ridge meets the warm advection east of the low. An example of such a scenario is diagrammed in the simplified 700 mb schematic of Figure 2. In such a case, enhanced precipitation south of this frontogenetical zone is quite common.

What happens, though, when this scene shifts slightly over your forecast area? For instance, suppose that the ridge shown in Figure 2 to the west of the split strengthened eastward. At the same time, cold advection around the back side of the low brought very cold air into the low, which became cut off from the main westerlies. Such a scenario is shown in the simplified 700 mb schematic of Figure 3. In such a case, the flow from the north is out of the warm core high, yielding warm advection through that area. The flow from the south is actually cold advection emanating from a cold pool of air within the closed low. Where, then, would the enhanced upward vertical motion due to the secondary circulations exist in this case? The enhanced upward motion is always on the warm side of the frontogenetic zone; therefore, the enhanced upward motion would be on the north side of the deformation axis.

Consider the case of 24 September 1987, a day when this "upside-down" deformation axis occurred. Figure 4 shows the 700 mb plot. The axis of dilatation stretches across southern Nevada and Utah. Considerable moisture exists south of this axis east of the closed low. Flow from the southwest into the axis suggests cold advection while flow from the north into the axis represents warm advection. Even though thermal advection is weak in this case, any contribution to the total vertical motion flow field by this deformation advection pattern should enhance upward vertical motion north of the axis and suppress it south of the axis. It is apparent, however, that the highest dew point temperatures, high relative humidities, and upward motion exist to the south of the axis. Does this make sense, physically?

Let's look at this case some more. The 18Z SIM graphic from the same day depicts a deformation axis across northern Utah as shown in Figure 5. This looks reasonable when compared to the 12Z IR satellite image (Figure 6) and the analyzed 700 mb chart. This axis was drawn in based primarily on the cloud locations and movement. Was it reasonable to place the deformation axis as shown in the SIM message?

Diagnosis and physical interpretation of this situation was really much simpler than normal in cases involving deformation axes. Quite often, especially during the warm season, convection will break out south of the deformation axis due to the enhanced upward vertical motion in that area. In such cases, it is often rather difficult to assess the degree to which the deformation axis will enhance the convection and precipitation. It should be clear to the meteorologist that the clouds and precipitation extending from southern Nevada and Utah and into northern Arizona have nothing whatsoever to do with forcing from the deformation axis in this case. The secondary upward vertical motion north of the deformation axis was much weaker than the synoptic scale subsidence south of the upper level high; hence, the dew point depressions across northern Nevada and Utah are rather high. The area of clouds and precipitation south of the deformation axis were likely due to the progression of a short wave on the east side of the closed low (indicated on Figures 5 and 7). The secondary circulations associated with the deformation axis actually acted to neutralize the vertical motion.

The placement of the deformation axis on the SIM graphic was not unfounded. The axis existed, and may have provided a good clue as to the boundary between the subsidence of the warm core high and the effects of the short wave. It was not, however, the primary impetus for the enhanced vertical motion as is so often the case across the West during the convective season. Although seemingly related to the deformation zone, the relative humidity analysis suggests that the total vertical motion field south of the deformation axis was dominated by the vorticity advection and not the frontogenetical axis.

The forecaster should, as much as possible, diagnose and understand the causes of the vertical motion pattern at the initial analysis time. Improper or incomplete understanding of the processes taking place can only lead to further errors when formulating a mental picture of future developments. This case illustrates how easy it can be to err in the diagnosis stage of the forecast, and how careful one must be to ensure that the diagnosis is correct.

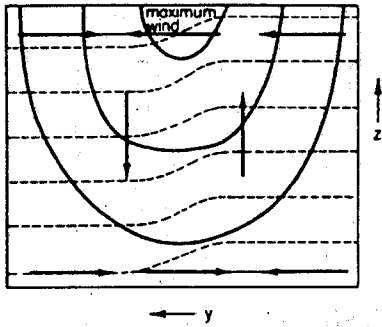


Figure 1. Vertical section across the axis of dilatation showing isotachs (solid), isotherms (dashed) and secondary circulation (arrows). After Sawyer (1956).

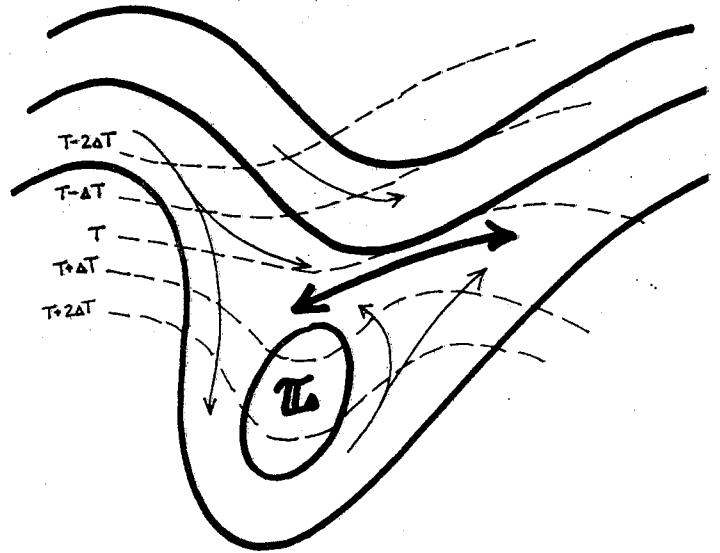


Figure 2. Simplified schematic of 700 mb heights (heavy solid), temperatures (dashed), streamlines (light arrows) and deformation axis of dilatation (heavy arrow). Enhanced upward motion is south of the deformation axis.

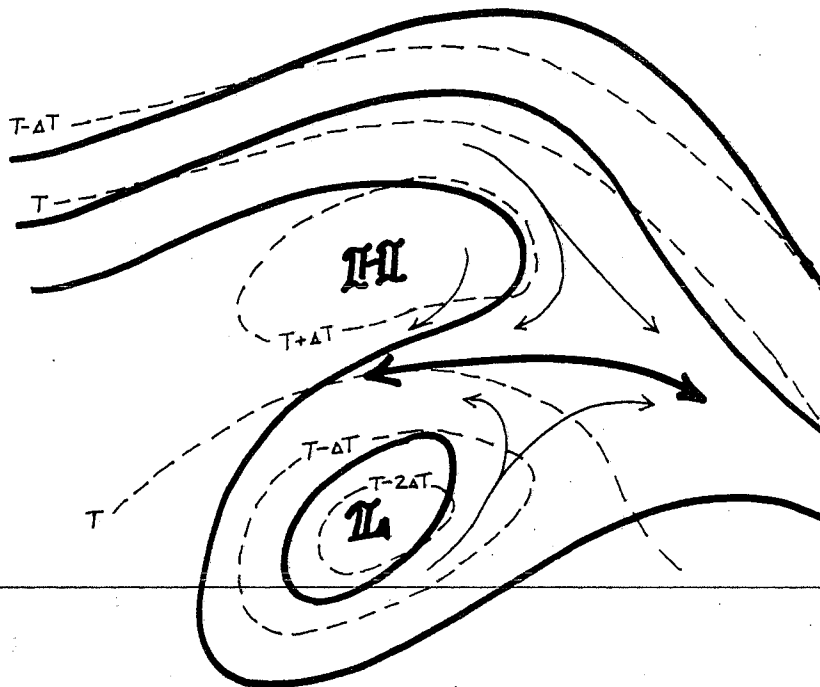


Figure 3. As in Figure 2, except enhanced upward motion is north of the deformation axis.

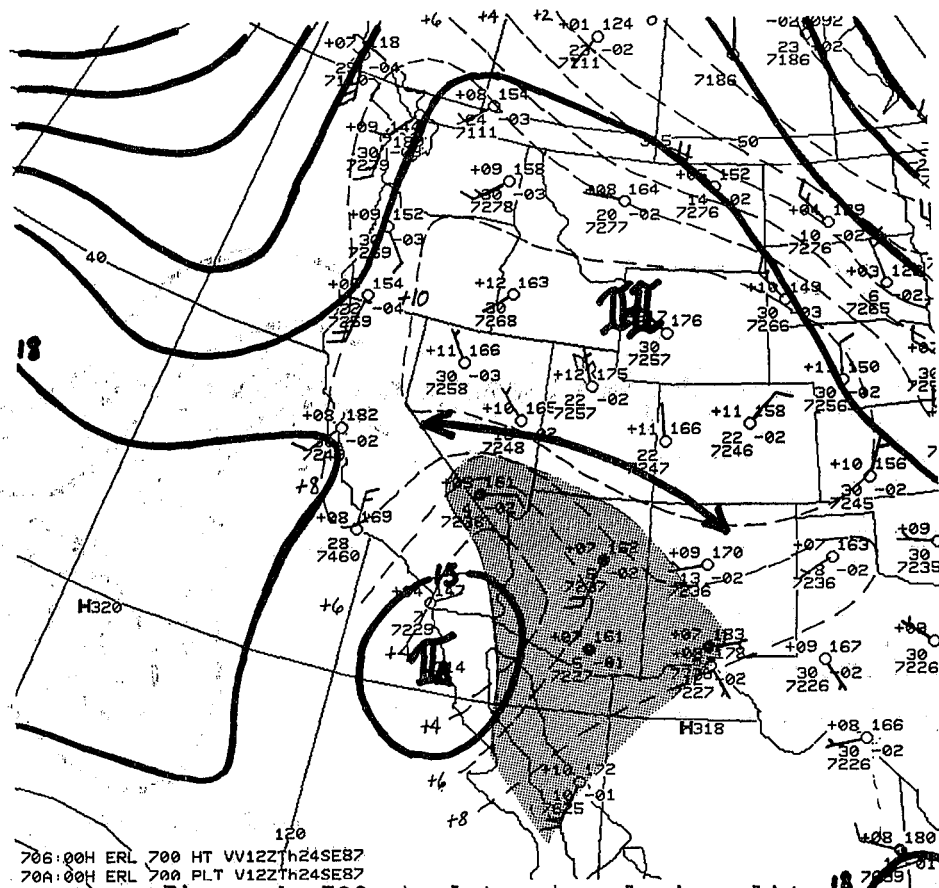


Figure 4. 700 mb plot and analysis valid 12Z 24 September 1987. Height, temperature and deformation axis as in Figure 2. Shading indicates dew point temperatures greater than -3C.

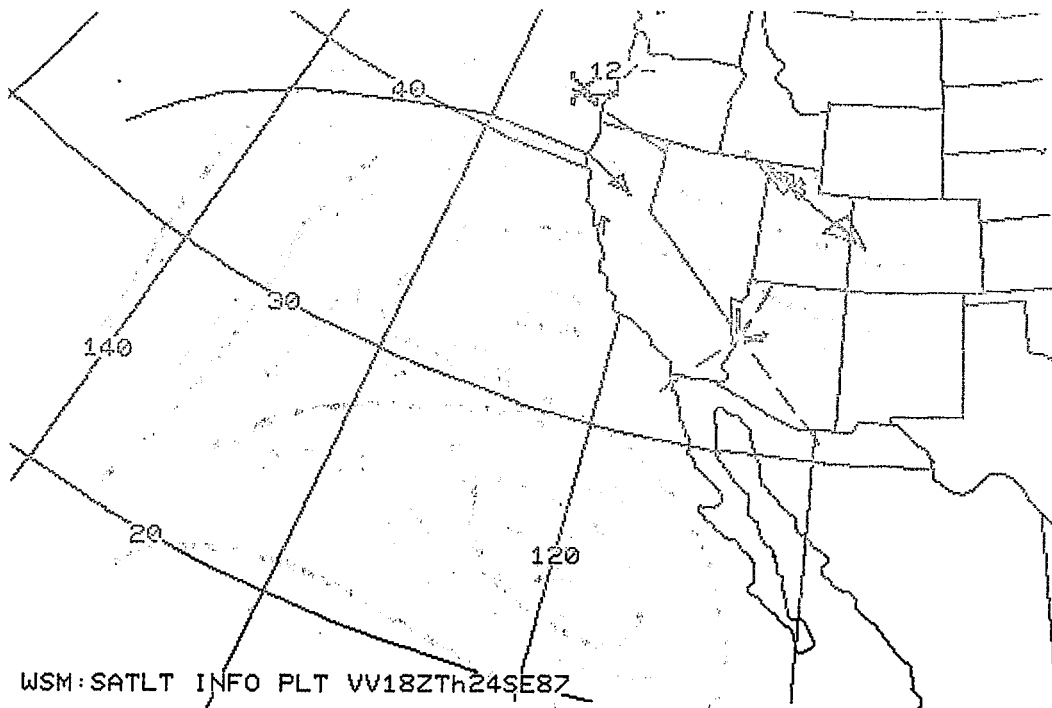


Figure 5. SIM graphic valid 18Z 24 September 1987.

1145 24SE87 28E-2HF 01012 23412 WB1

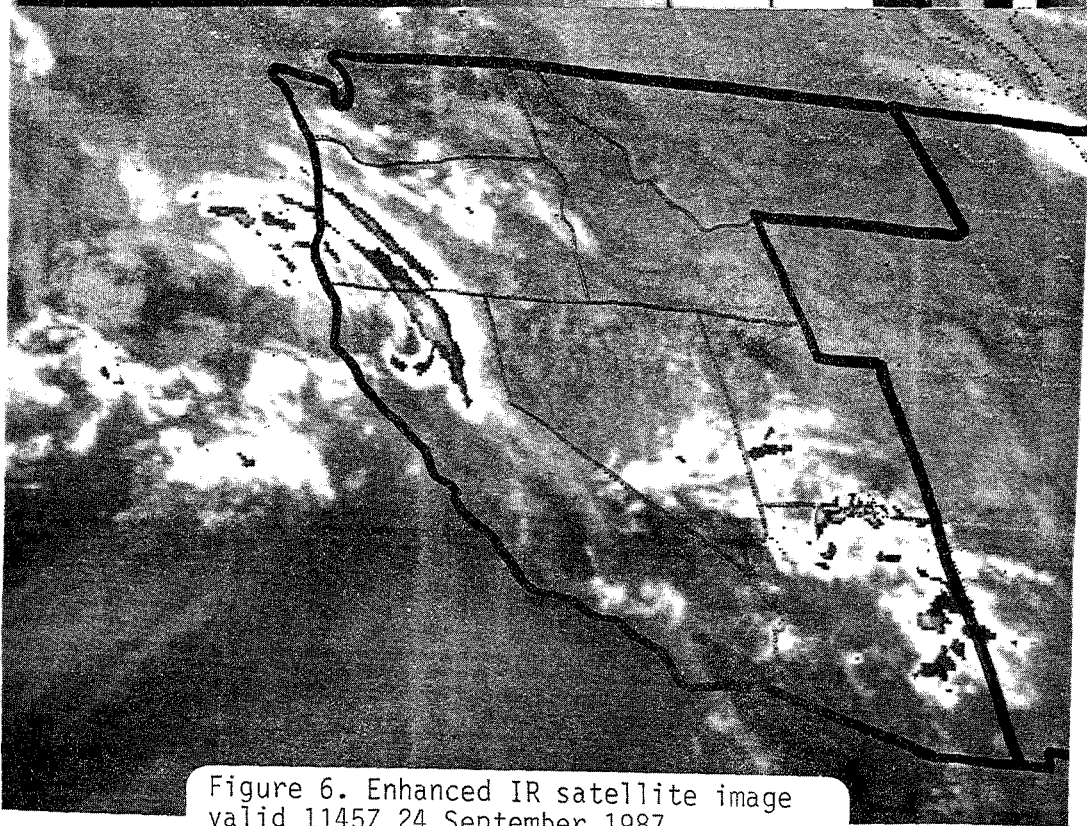


Figure 6. Enhanced IR satellite image valid 1145Z 24 September 1987.

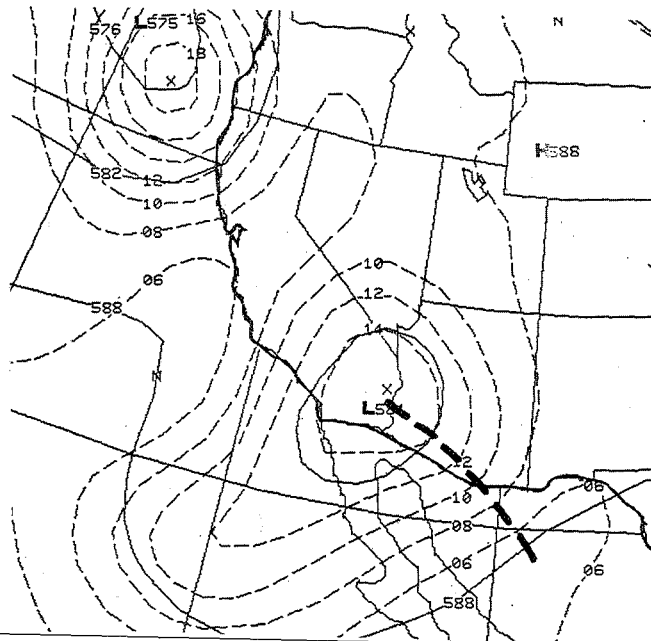


Figure 7. NGM 500 mb height and vorticity initial analysis valid 12Z 24 September 1987.